
PHYSICS OF ELEMENTARY PARTICLES
AND ATOMIC NUCLEI. EXPERIMENT

Simulation of Neutronics of an Accelerator Driven System

A. I. Dubrouski^{a,*} and A. I. Kiyavitskaya^a

^aInternational Sakharov Environmental Institute, Belarusian State University, Minsk, 220070 Belarus

*e-mail: a1dubrovskii@gmail.com

Received August 30, 2019; revised September 1, 2019; accepted September 20, 2019

Abstract—Experiments with a big uranium target irradiated by a high-energy proton beam will be carried out at JINR (Dubna, Russia). In this paper, a number of neutronics of this accelerator-driven subcritical system are simulated towards optimizing the experimental conditions. The Geant4-based simulations are performed in the International Sakharov Environmental Institute of Belarusian State University.

DOI: 10.1134/S1547477120010069

INTRODUCTION

Today, synergic systems aimed at nuclear-waste transmutation and energy generation [1, 2] are being developed in all countries that rely on nuclear energy. Synergic systems are viewed as the most promising approach to reprocessing of long-lived fission fragments and minor actinides. In such a system, a complete production chain is obtained by combining different technologies, including nuclear ones (those of nuclear fission, fusion, and spallation induced by high-energy particle beams). The concept of an accelerator-driven system (ADS) has been developing since the 1990s [3]. In this, a high-energy beam from a particle accelerator is used for inducing large-scale spallation reactions in an extended heavy target whereby neutrons are produced. Upon breeding in a subcritical blanket ($k_{\text{eff}} \sim 0.9\text{--}0.98$), they induce the fission of uranium nuclei. A high neutron flux thereby produced ($\Phi \sim 10^{15\text{--}17}$ neutron/(cm²s)) can be employed for generating energy, transmuting radioactive isotopes, and producing tritium for thermonuclear sources [1–3].

The basic concept of any ADS is to employ a high-energy particle accelerator for generating spallation neutrons in a heavy target (Pb, Bi, W, U, Pb–Bi eutectic), which then are bred through the chain nuclear reaction. Such a subcritical system comprises a high-energy proton accelerator, a spallation target, a subcritical blanket with a multiplication factor of $M = 1/(1 - k_{\text{eff}}) \sim 50$, a steam generator, a turbine, and an electrogenerator. As soon as the accelerator operation is halted, neutrons from the spallation target no longer enter the nuclear fuel and the chain fission reaction almost instantly dies down. Constructing an operating ADS poses a number of physical and technical problems: one has to (i) optimize the proton-beam energy and current and construct an accelerator with the requisite parameters, (ii) select the target material and optimize its design towards producing the required

amount of spallation neutrons, (iii) develop the scheme of heat transfer from the target block, (iv) work out the design of the subcritical blanket consistent with nuclear safety, (v) develop the scheme of heat transfer from the subcritical blanket, and (vi) estimate the transmutation and accumulation rates for the long-lived nuclides [1–3]. At present, optimizing the neutron energy spectrum towards efficiently transmuting the long-lived fission fragments (iodine, cesium, strontium, zirconium) and minor actinides (neptunium, plutonium, americium, curium) still remains an important open problem despite a large number of available theoretical analyses. Primarily, this is because the cross sections for neutron interactions with radioactive nuclei over the broad energy range between 1 eV and 10 GeV are not known to the required precisions. Resolving this problem will significantly affect the process of ADS practical realization. On the other hand, since the k_{eff} value must be maintained at a required level for a blanket consisting of different nuclides, a definite approach to experiments with subcritical targets, including their nuclear and radiation safety, should be formulated.

Experiments with a big uranium target irradiated by high-energy protons are scheduled at the Joint Institute for Nuclear Research (Dubna) [4]. Calculations of neutronics of a big uranium target with different spallation targets were carried out back in the 1990s and reported in [5] (actually, these referred to a reactor based on muon-catalyzed fission). In this paper, the results obtained in [5] are compared with those of a Geant4-based simulation [6].

SETUP DESCRIPTION

The uranium target is assumed to be a cylinder with 120-cm external diameter and 100-cm thickness along the beam. The beam passes through a 6-cm-wide and 40-cm-long channel starting at the target upstream face and impinges on the spallation target inserted in a

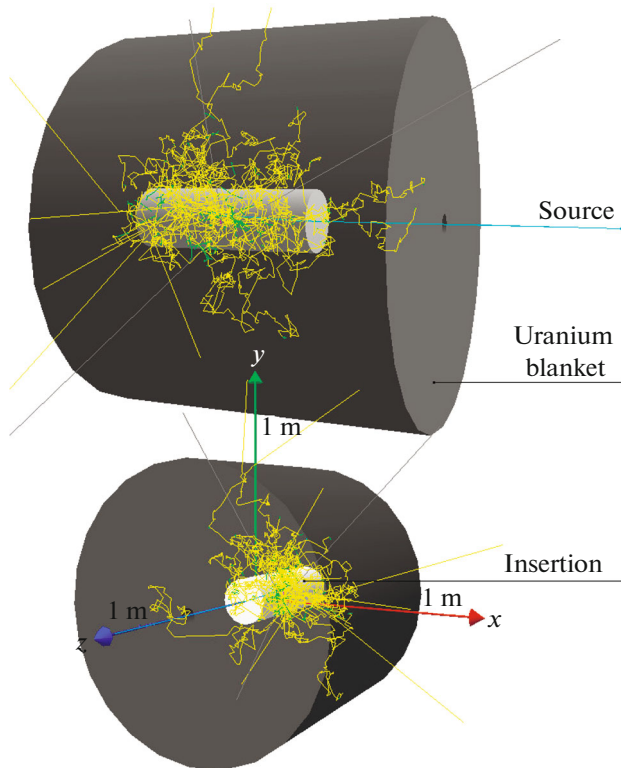


Fig. 1. Model of the big uranium target.

20-cm-wide and 60-cm-long opening extending to the downstream face of the uranium target (see Fig. 1).

The blanket consists of depleted uranium containing 0.4% of ^{235}U , which corresponds to the ^{238}U and ^{235}U volume densities of 0.0471×10^{24} and $0.000189 \times 10^{24} \text{ cm}^{-3}$, respectively.

SIMULATION

Propagation of a high-energy particle or nucleus through matter proceeds in two distinct stages which involve different reactions producing secondary particles of different types and energies [1, 6, 7]. At the first stage, secondary hadrons are massively produced in hard nuclear collisions and then propagate through matter. At the second stage, low-energy neutrons ($E_n \leq 20 \text{ MeV}$) produced in fission and spallation reactions propagate through matter. Therefore, for our purposes, the simulation of the internuclear cascade reduces to identifying and characterizing the sources of low-energy neutrons with $E_n \leq 20 \text{ MeV}$ (including their energy and angular distributions) and then simulating the process of neutron transfer relying on the methods known from the nuclear-reactor theory.

For a particle with energy in the MeV and GeV ranges, interaction with matter is a complex process involving the emission of different strongly interacting particles (protons, neutrons, pions, etc.); electromag-

netic interactions; nuclear reactions; and the formation and development of an electromagnetic cascade and, at subsequent stages, complex chains of chemical reactions [1, 6, 7].

The interaction process as a whole can be divided into definite time stages determined by corresponding interaction mechanisms, characteristic durations of nuclear reactions, transfer mechanisms for the high- and low-energy heavy nuclear fragments, and the properties of chemical reactions that occur throughout the interaction process of high-energy radiation with matter. Depending on the type and energy of the primary particle and on the medium properties, the characteristic interaction time varies from some 10^{-21} s up to milliseconds and even minutes for fissionable media.

The primary collision with the target nucleus induces a series of prompt reactions referred to as the intranuclear cascade, whereby separate nucleons and nucleon clusters are knocked out of the nucleus. As soon as the energy is above a few GeV per nucleon, fragmentation of the nucleus occurs. The intranuclear cascade leaves the target nucleus in an excited state, which gradually relaxes to the ground state through γ emission and the evaporation of nucleons and light nuclei ($n, p, d, t, {}^3\text{He}, {}^4\text{He}$), where neutron evaporation plays a dominant role [1, 6, 7]. In a thick target, energetic secondary particles with $E > 20 \text{ MeV}$ induce spallation reactions. In some target materials, low-energy secondary spallation neutrons with $E < 20 \text{ MeV}$ (those emitted at the cascade and evaporation stages) can induce the (n, xn) reactions. For a heavy-element target, evaporation can be accompanied by the competitive process of high-energy induced fission of strongly excited nuclei [1, 6, 7]. High-energy fission can occur in the tantalum, tungsten, lead, thorium, and depleted-uranium targets. In the latter two, fission can be also induced by neutrons with energies below 20 MeV. These complex processes are simulated using dedicated computer algorithms (LAHET, HETC, SONET, SPECTR, FLUKA, Geant4, etc.) developed at the world's leading laboratories.

The simulations reported in this paper employ the QGSP_BIC_HP standard physical model implemented in the Geant4 package. In describing particle interactions, this model relies on the cross-section data compiled in the ENDF open library (Evaluated Nuclear Data File). This scheme adequately describes the development of intranuclear cascades, including time and energy dependences, and comprises the following basic constituents:

- QGSP (Quark-Gluon String Precompound)—the quark-gluon string model for describing the high-energy proton, neutron, pion, and kaon collisions with nuclei;
- BIC (Binary Cascade)—the binary cascade model, whereby the production of secondary particles in proton and neutron interactions with nuclei at energies up to 10 GeV is adequately described;

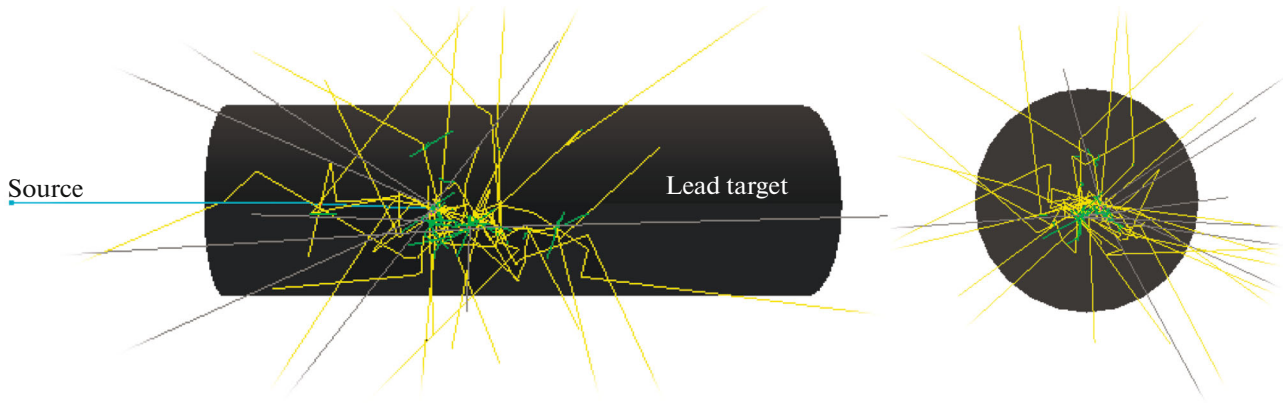


Fig. 2. Scheme of the lead spallation target with $R = 20$ cm and $L = 60$ cm.

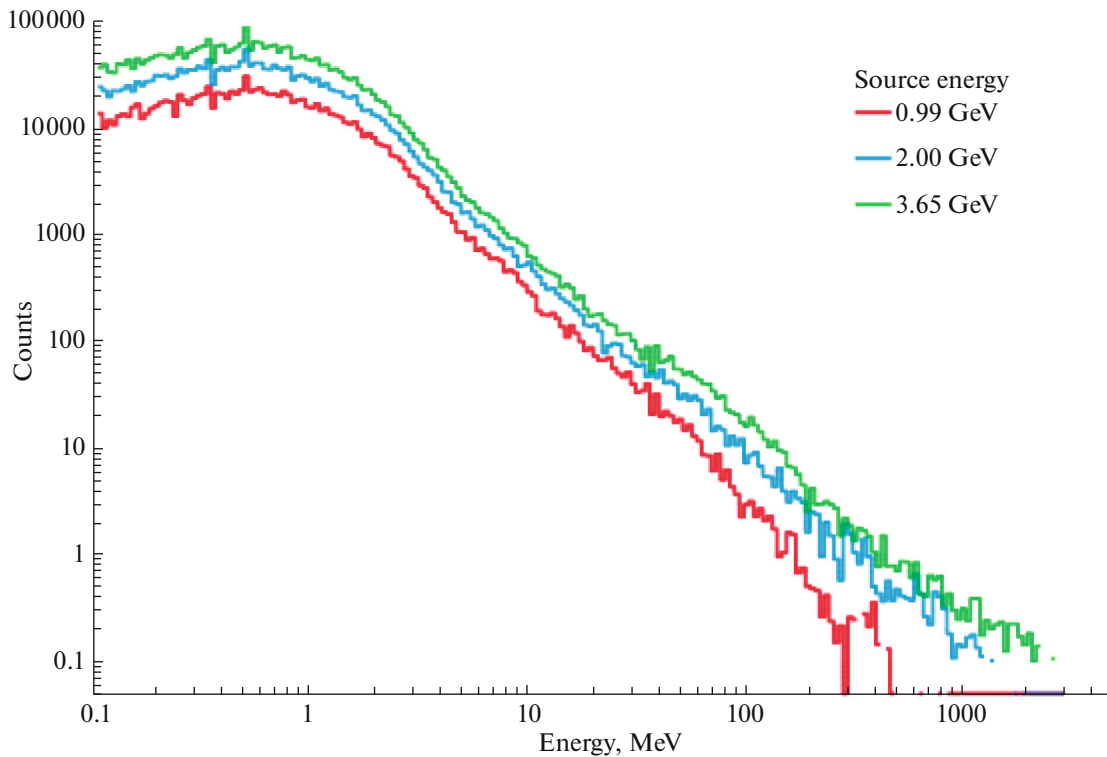


Fig. 3. Energy spectra of neutrons emitted from the lead spallation target with $R = 20$ cm and $L = 60$ cm for different energies of incident protons.

- NeutronHP (Neutron High Precision)—the high-precision interaction model for neutrons with energies below 20 MeV [10].

The NeutronHP model is the Geant4 default code for describing the formation of fission fragments. In the latest Geant4 versions, the FFG (Fission Fragment Generator) code is implemented whereby the events of binary and triple fission are accurately described, including the fragment masses and energies [11]. Both fission models are employed in the reported simulations.

DISCUSSION OF RESULTS

The first step is to compare our predictions for neutron emission from a lead spallation target with the measurements [12, 13]. We find that our simulation adequately reproduces the measured total yields [12] and energy spectra [13] of neutrons emitted from the lead target (see Table 1).

With increasing proton energy, the mean number of collisions and the net neutron yields increase, while the shape of the neutron energy spectrum remains practically the same (see Fig. 3).

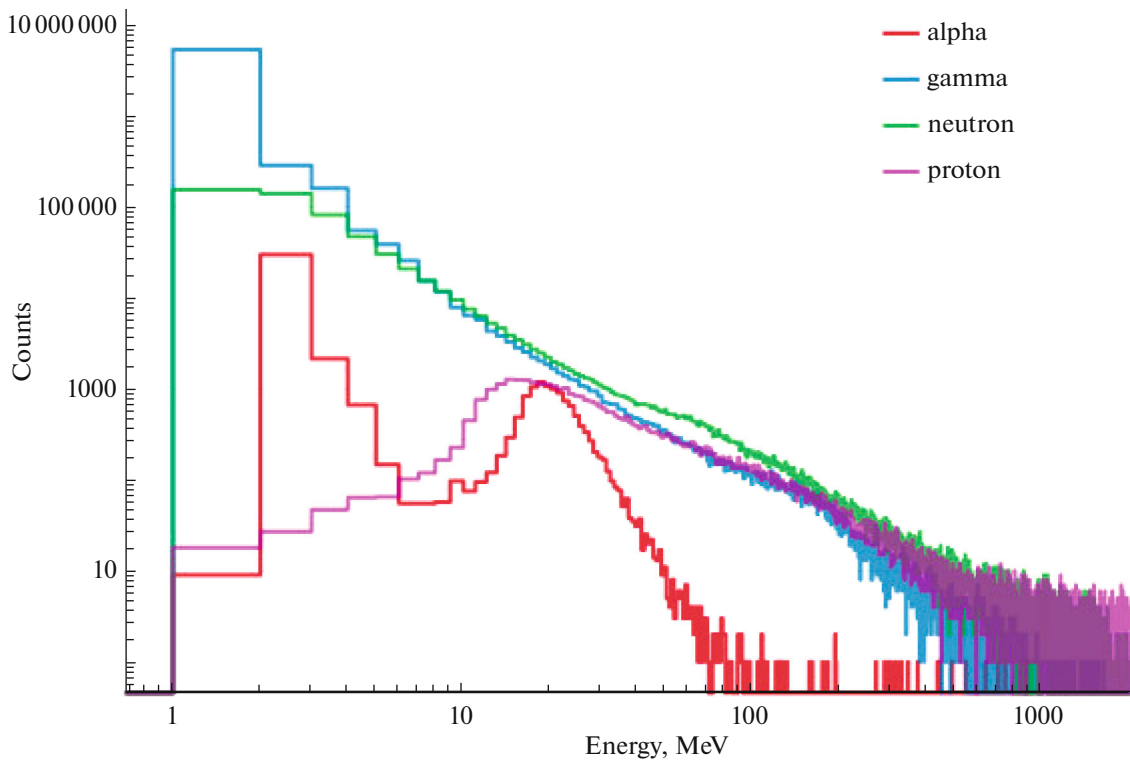


Fig. 4. Energy spectra of different secondary particles produced within the lead spallation target.

Simulated kinetic-energy distributions of different particles produced within the spallation target and of those emitted from the target are shown in Figs. 4, 5 and Figs. 6, 7 for the lead and beryllium targets, respectively (10^4 events). The corresponding total yields per incident proton are compiled in Table 2. In the beryllium target, when compared to the lead one,

fewer secondary particles are produced but, on the other hand, their absorption is significantly weaker. The lead target shows a high yield of produced γ quanta (especially in the low energy range), but almost all soft γ quanta are absorbed inside the target. The γ quanta and protons emitted from the beryllium target have higher mean energies than those emitted from the lead target. The energy spectrum of α particles produced within the lead target features a peak near 20 MeV arising from the $^{107}\text{Pb}(p,\alpha)^{204}\text{Tl}$ reaction. That the yield of produced neutrons including the energetic ones is significantly higher for the lead target is probably due to neutron breeding via the high-energy (p, xn) and ($p, \text{fission}$) reactions (the fission barrier is near 24 MeV for lead).

The distributions in the numbers of different secondary particles produced in the big uranium target with inserted Be and Pb spallation targets are shown in

Table 1. Measured and simulated neutron yields per incident proton from a lead spallation target with $R = 20$ cm and $L = 60$ cm

Beam energy, GeV	Data [12]	Geant4
0.991	25.1 ± 3.0	25.9448
2.0	44.2 ± 3.1	50.7262
3.65	80.7 ± 6.9	84.9362

Table 2. Secondary particles yield per one incident proton for different targets

Target material	Particle yield per proton	α particles	γ quanta	neutrons	protons
Be	Produced in the target	4.5950	6.2372	5.5912	4.0138
	Emitted from the target	0.0002	4.3485	3.9630	0.9220
Pb	Produced in the target	4.4025	601.3480	61.9083	6.4625
	Emitted from the target	0.0002	5.6004	42.4793	0.1786

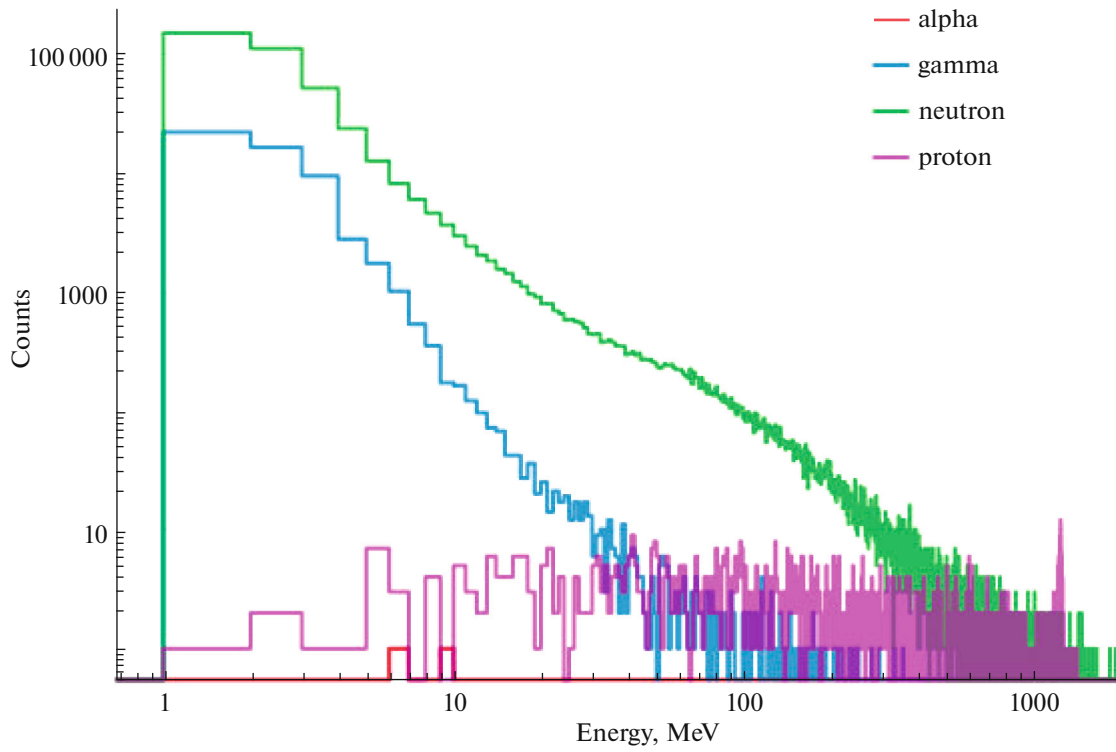


Fig. 5. Energy spectra of different secondary particles emitted from the lead spallation target.

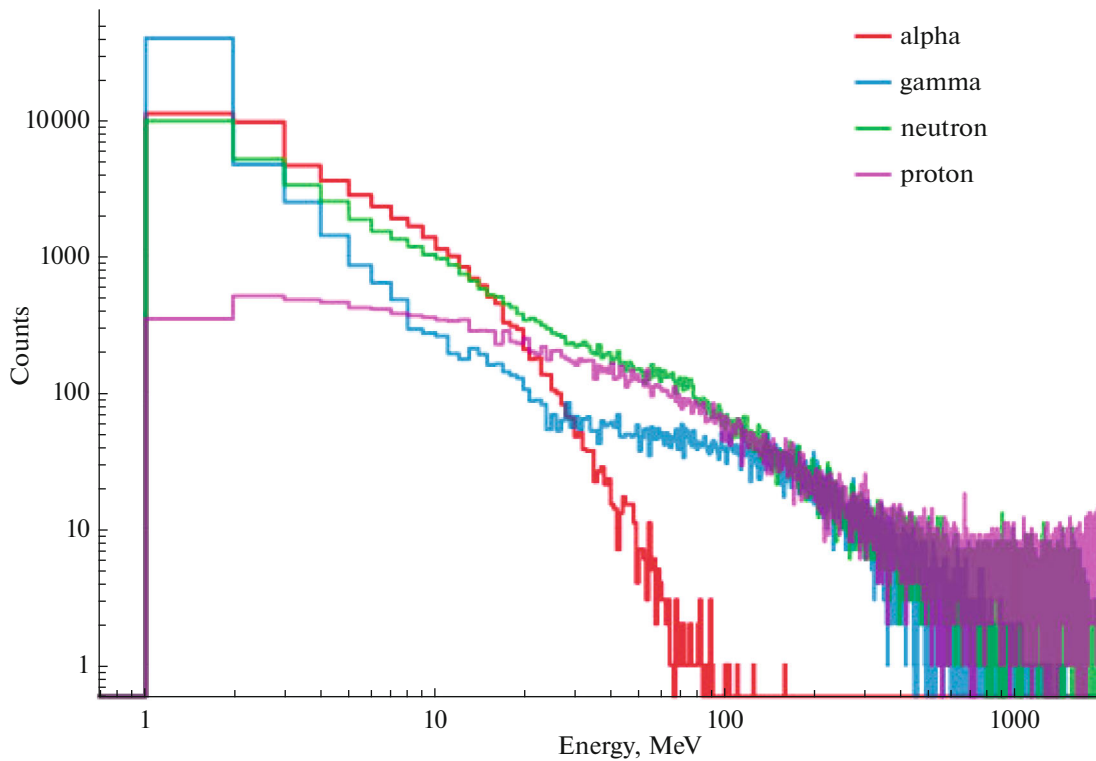


Fig. 6. Energy spectra of different secondary particles produced within the beryllium spallation target.

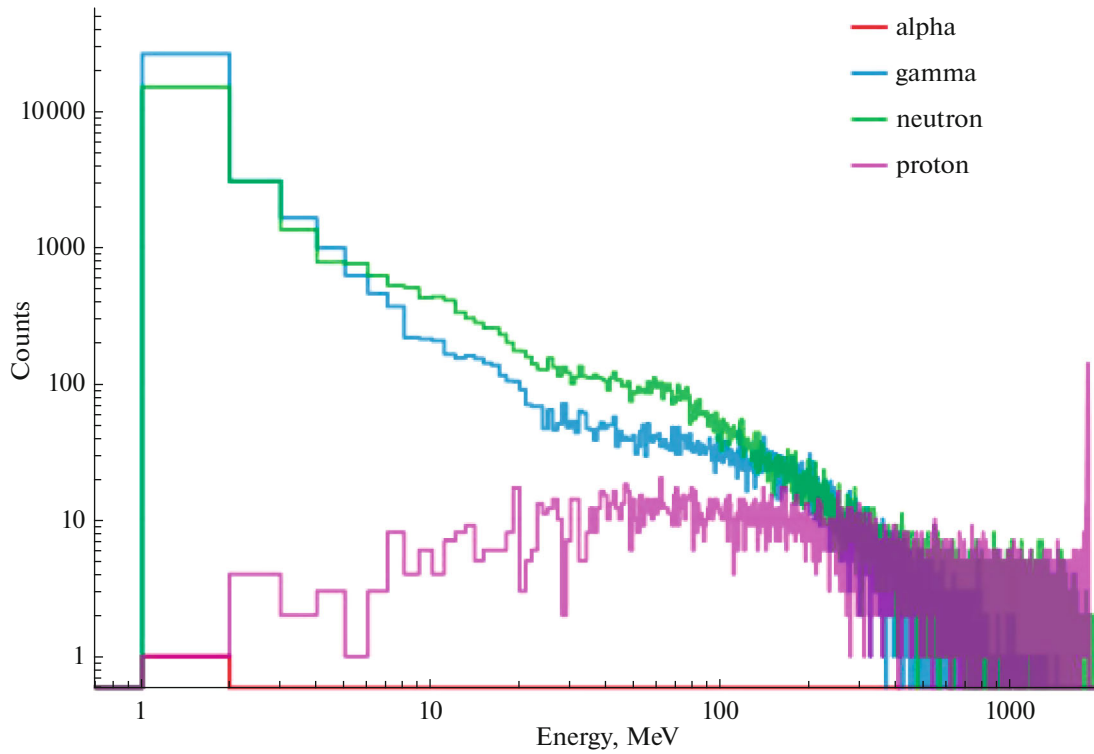


Fig. 7. Energy spectra of different secondary particles emitted from the beryllium spallation target.

Figs. 8 and 9, respectively (these are normalized to one incident 2-GeV proton). A single proton-induced event is seen to involve up to 20 secondary protons largely produced within the spallation-target volume. By the moment the chain fission reaction terminates, the total number of produced neutrons varies between 0 and 2000. Since more secondary particles are pro-

duced in the Pb spallation target than in the Be one, the maximums of the distributions shown in Fig. 9 are shifted to higher particle multiplicities when compared to those of Fig. 8.

In Table 3, previous estimates [5] of the neutron-production characteristics of the big uranium target with inserted beryllium and lead spallation targets irradi-

Table 3. Neutronics of the big uranium target

Normalized to one beam particle	Be spallation target			Pb spallation target		
	Results [5]	Geant4 FFG	Geant4 NeutronHP	Results [5]	Geant4 FFG	Geant4 NeutronHP
Effective multiplication factor k_{eff} for neutrons with $E < 10.5$ MeV	0.42	0.61	0.544	0.36	0.492	0.428
Number of secondary fission neutrons in the low-energy region	33.3	31.81	25.479	47.6	62.083	49.871
Number of $(n, 2n)$ reactions in the low-energy range	2.47	2.831	2.314	1.6	2.668	2.041
Number of low-energy neutrons captured by the nuclei of all elements	54.8	40.908	36.557	96.5	103.45	94.771
Number of low-energy fissions	12.2	10.121	10.067	17.1	19.659	16.035
Number of low-energy fissions for ^{238}U	9	7.409	5.801	14.1	16.388	13.032
Number of inelastic collisions of high-energy particles in the spallation target	3.16	2.974	2.931	—	8.085	7.972

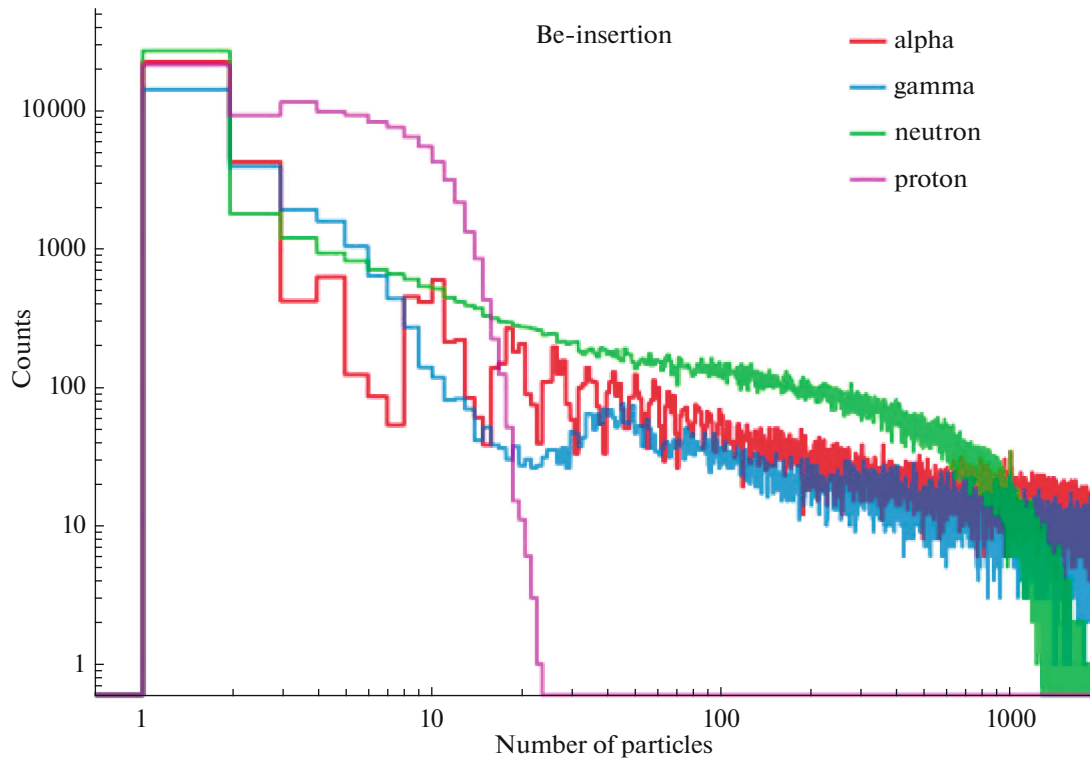


Fig. 8. Distributions of the numbers of different particles emitted within the system with Be-insertion for a beam energy of 2 GeV.

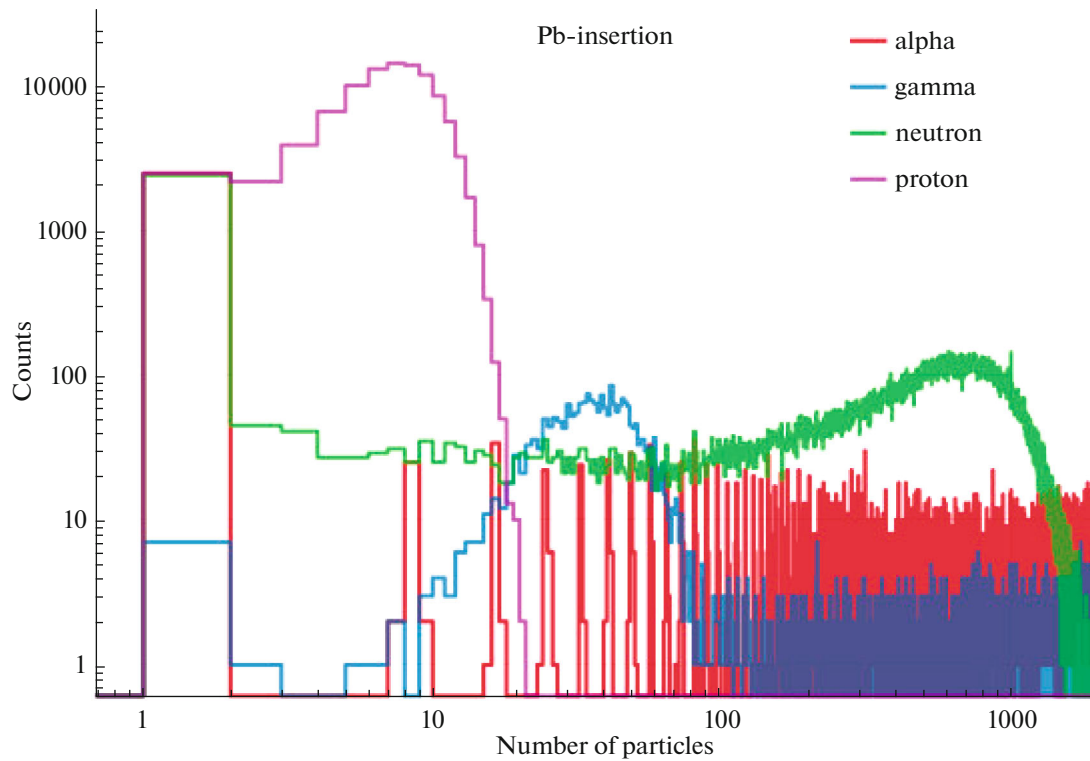


Fig. 9. Distributions of the numbers of different particles emitted within the system with Pb-insertion for a beam energy of 2 GeV.

ated by 2-GeV protons are compared with the results of our Monte-Carlo simulation. The calculation reported in [5] relied on the SONET code [7], which involves model descriptions of inter- and intranuclear cascades at the high-energy stage; the nuclear breakup and evaporation models for $A < 20$ and $A > 20$, respectively; and the Fong model for high-energy fission [5–8].

Note that, in analyses [5, 7–9], some important factors were neglected: thus, the proton beam was assumed to be strictly normal to the target, the target was assumed to be homogeneous, and the layout of measuring devices was not taken into account. Apart from that, the computers available at that time would not allow for carrying out precise numerical calculations. This may explain why the calculations based on the SONET code [7] and on the Geant4 simulation package yield different predictions for the physical characteristics of the big uranium target with inserted beryllium and lead spallation targets. Note that the predictions based on the high-precision model of neutron interactions are the closest to those of analysis [5] in the energy range below 20 MeV [10] while underestimating the reaction rates and neutron yields for the beryllium target when compared to [5].

The simulations were carried out using the Intel Core i7-6700 processor with a clock frequency of 3.4 GHz and 8 Gb RAM. It took about 20 h of real time to perform 10^5 events in multithreading mode. Geant4 10.05.p01 version was used for simulation. Presented on the histograms data was obtained using QGSP_BIC_HP standard physics list without the FFG option.

CONCLUSIONS

Preliminary results of the numerical investigation of neutronics of a subcritical system irradiated by a high-energy particle beam are reported using the JINR big uranium target as an example. At this stage of simulation, the geometry of the experimental hall housing the subcritical target and the accelerator is not taken into account. Our simulation adequately reproduces the measured yields and energy spectra of neutrons emitted from a lead spallation target.

For the JINR big uranium target as a whole, the results of our Geant4-based simulations are compared with those of previously performed calculations that relied on a combination of the SONET and MCNP4A computer codes. Some disagreements between the present and previous predictions are revealed, and their possible origins are discussed.

Towards a better understanding of the subcritical-system kinetics, the simulation procedure will be upgraded by including the detailed geometry of the experiment and refining the physical models employed. This will render our predictions more reliable and help formulate the scientific goals of the experiments with a big uranium target to be carried out at JINR.

REFERENCES

1. H. Kiyavitskaya, V. Bournos, I. Serafimovich, C. Routkovskaya, and Y. Fokov, “Transmutation of fission products and minor actinides in a subcritical assembly driven by a neutron generator,” in *Proceedings of the NATO Advanced Research Workshop: Nuclear Science and Safety in Europe, Yalta, Ukraine, Sept. 10–16, 2005, NATO Security through Science Series, Ser. B: Phys. Bio-phys.* (Springer, Dordrecht, 2006).
2. A. I. Kievitskaya, “Neutron-physical characteristics of subcritical systems: YALINA stand,” Doctoral (Phys. Math.) Dissertation (Minsk, 2017).
3. M. Salvatores et al., “Global physics approach to transmutation of radioactive nuclei,” *Nucl. Sci. Technol.* **116**, 215–227 (1994).
4. A. A. Baldin, A. I. Berlev, I. V. Kudashkin, G. Mogildea, M. Mogildea, M. Paraipan, and S. I. Tyutyunnikov, “Simulation of neutron production in heavy metal targets using Geant4 software,” *Phys. Part. Nucl. Lett.* **13**, 249 (2016).
5. A. I. Kievitskaya, “Mesocatalytic hybrid reactor. Neutron-physical characteristics and energy balance,” Cand. Sci. (Phys. Math.) Dissertation (Minsk, 1991).
6. V. S. Barashenkov and V. D. Toneev, *Interactions of High-Energy Particles and Atomic Nuclei with Nuclei* (Atomizdat, Moscow, 1972) [in Russian].
7. S. Chigrinov, I. Rakhno, and H. Kiyavitskaya, “The code SONET to calculate accelerator driven system performance,” in *Proceedings of the 3rd International Conference on Accelerator Driven Transmutation Technologies and Application (99’ADTTA), Praha, Pruhonice, Czech Republic, June 7–11, 1999*, MO-O-C12, pp. 1–8.
8. A. Kievitskaia, I. Rakhno, and A. Kievitskaia, “Monte Carlo calculation of relativistic protons interaction with extended targets and transmutation of iodine-129 and neptunium-237,” in *Proceedings of the International Conference on the Physics of Nuclear Science and Technology, New York, October 5–8, 1998*, pp. 1455–1461.
9. S. Chigrinov, A. Kievitskaia, and V. Petlitskij, “Relevance of mesocatalytic hybrid reactors for accumulation of fissile nuclei and energy balance analysis,” *Nucl. Fusion* **33**, 815 (1993).
10. Geant4 Use Cases—Reference Physics Lists. <https://Geant4.web.cern.ch/node/302>. Accessed July 1, 2019.
11. B. Wendt and E. Burgett, “Development and integration of a fission event generator into the Geant4 framework,” in *Proceedings of the Student Conference, Pennsylvania, USA, April 3–5, 2014* (Am. Nucl. Soc., 2014).
12. M. S. Zucker et al., “Spallation neutron production measurements,” in *Proceedings of the 2nd International Conference on Accelerator Driven Transmutation Technologies and Applications (ADTTA), Kalmar, Sweden, June 1996*, Vol. 1, pp. 527–533.
13. O. Grudzevich and S. Yavshits, “Complete files of neutron- and proton-induced nuclear data to 1 GeV for 208Pb target,” in *Proceedings of the 8th International Conference on Nuclear Data for Science and Technology, Nice, France, April 22–27, 2007*, p. 102.

Translated by A. Asratyanl